

# Vibrations due to a test train at variable speeds in a deep bored tunnel embedded in London clay

G. Degrande<sup>a,\*</sup>, M. Schevenels<sup>a</sup>, P. Chatterjee<sup>a</sup>, W. Van de Velde<sup>a</sup>, P. Hölscher<sup>b</sup>,  
V. Hopman<sup>b</sup>, A. Wang<sup>c</sup>, N. Dadkah<sup>d</sup>

<sup>a</sup>Department of Civil Engineering, K.U. Leuven, Kasteelpark Arenberg 40, B-3001 Leuven, Belgium

<sup>b</sup>GeoDelft, P.O. Box 69, ATP, Stieltjesweg 2, 2600 AB Delft, The Netherlands

<sup>c</sup>Pandrol Rail Fastenings Ltd, 63 Station Road, Addlestone, Surrey KT15 2AR, UK

<sup>d</sup>London Underground Ltd, 84 Eccleston Square, London SW1V 1PX, UK

Accepted 26 August 2005

Available online 7 February 2006

---

## Abstract

This paper reports on the results of in situ vibration measurements that have been performed within the frame of the CONVURT project at a site in Regent's Park on the Bakerloo line of London Underground during 35 passages of a test train at a speed between 20 and 50 km/h. Vibration measurements have been performed on the axle boxes of the test train, on the rails, on the tunnel invert and tunnel wall, and in the free field, both at the surface and at a depth of 15 m. Measurements have also been made on floors and columns of two buildings in a row of Regency houses at a distance of 70 m from the tunnel. Prior to these vibration measurements, the dynamic soil characteristics have been determined by in situ and laboratory testing. Rail and wheel roughness have been measured and the track characteristics have been determined by rail receptance and wave decay measurements. Time histories and one-third octave band RMS spectra of the measured velocities are discussed and the variation of the peak particle velocity and the frequency content as a function of the train speed and the distance to the tunnel are elaborated.

© 2006 Elsevier Ltd. All rights reserved.

---

## 1. Introduction

The main objective of this paper is to describe the results of elaborate in situ vibration measurements that have been performed within the frame of the CONVURT project [1] at a site in Regent's Park situated above the north- and south-bound Bakerloo line tunnels of London Underground. These tunnels are deep-bored segmented tunnels with a cast iron lining and a single track, embedded in London clay at a depth of 28 m. The vibration measurements have been carried out on a straight section of the north-bound Bakerloo line. The reference section is situated at kilometre post 46.306 (Fig. 1), which is 581 m west of Regent's Park station, or approximately 200 m east of Baker Street station. The measurement site is surrounded by a boating lake to the

---

\*Corresponding author. Tel.: +32 16 32 16 67; fax: +32 16 32 19 88.

E-mail address: [geert.degrande@bwk.kuleuven.be](mailto:geert.degrande@bwk.kuleuven.be) (G. Degrande).

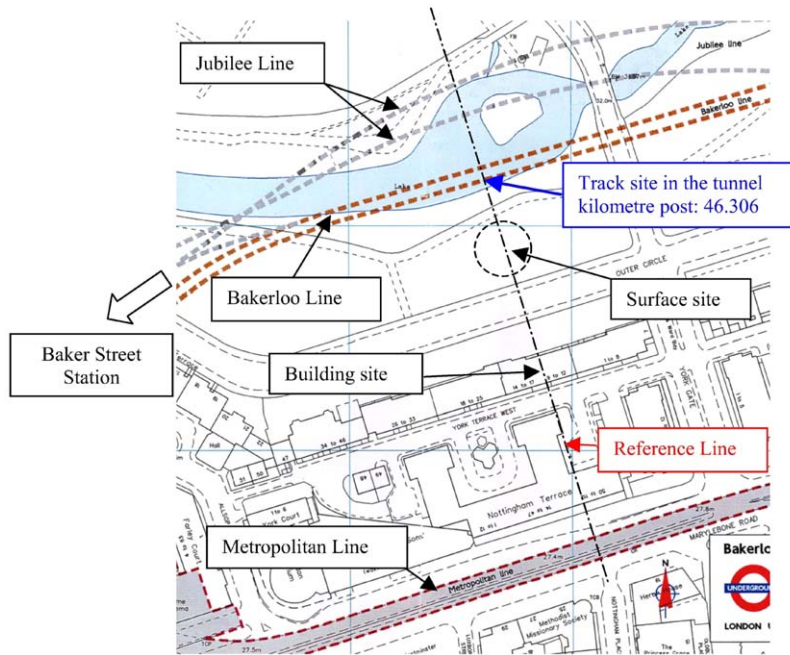


Fig. 1. Plan of the measurement site in Regent's Park.

north and by the Outer Circle to the south. A row of Regency houses is built along York Terrace West, parallel to the Outer Circle, at a distance of about 70 m from the north-bound Bakerloo line tunnel.

During service hours, trains running on the Bakerloo line could easily be differentiated from trains on the north- and south-bound Jubilee line and on the Metropolitan line (Fig. 1), as they give rise to the highest level of vibration, even in the buildings on York Terrace West that are relatively close to the shallow cut-and-cover tunnel of the Metropolitan line.

This paper concentrates on the vibration measurements that have been performed during engineering hours at night for 35 passages of an instrumented test train in the north-bound Bakerloo line tunnel at a speed between 20 and 50 km/h.

Vibration measurements have been performed on the axle boxes of the test train [2], on the rails [3], on the tunnel invert and tunnel wall [3] and in the free field, both on the surface and at a depth of 15 m, where tri-axial accelerometers have been installed in a seismic cone [4,5]. Measurements have also been made on several floors and columns of two buildings at 17 and 25 York Terrace West [4]. Both buildings are reinforced concrete frame structures with a repetitive structure parallel to the tunnel at a distance of about 70 m. During the experiments, the building on 25 York Terrace West was under renovation, involving important structural changes using steel columns and beams.

Apart from these vibration measurements, rail and wheel roughness have been measured, while the track characteristics have been determined by rail receptance measurements [3]. The dynamic soil characteristics have been determined by in situ tests (seismic cone penetration tests (SCPT), spectral analysis of surface waves (SASW)) and by laboratory testing on undisturbed samples (bender element test, free torsion pendulum test) [5,6].

The characteristics of the tunnel, the track, the train and the soil are first reviewed. Subsequently, the measurement setup and data analysis procedures are briefly outlined. Time histories and one-third octave band spectra of the velocity during the passage of the test train at various speeds are discussed. In particular, the variation of the peak particle velocity (PPV) and the frequency content as a function of the train speed and distance to the tunnel are elaborated. Furthermore, it is demonstrated how the vibrations are attenuated at the basement of the building and propagate into the building.

The results presented in this paper are complementary to the results of in situ tests that have been performed within the frame of the same project at a site in the Cité Universitaire on the line Réseau Express Régional (RER) B of Régie Autonome des Transports Parisiens (RATP) in Paris [7–10], where a shallow cut-and-cover tunnel with two ballasted tracks is embedded in sandy soil.

The results of the vibration measurements on both sites are presently being used to validate the modular numerical prediction models that have been developed within the framework of the project [11–16].

## 2. Characteristics of the tunnel and the track

The tunnel on the Bakerloo line is a deep-bored tunnel with a cast iron lining and a single track, embedded in London clay at a depth of about 28 m below the surface. The tunnel has an external radius of 1.953 m, while the thickness of the lining is 0.022 m. There are six longitudinal stiffeners (with a height of 0.102 m and a width of 0.057 m) and one circumferential stiffener at an interval of 0.508 m in the longitudinal direction, resulting in a periodic tunnel structure (Fig. 2).

The track in the tunnel is of the conventional London Underground type. It is a non-ballasted concrete slab track with a 95 lb Bullhead rail supported on hard Jarrah wooden sleepers nominally spaced at 0.95 m with cast iron chairs. The ends of a sleeper are embedded in the concrete invert, which runs along the sides of the floor of the tunnel and has a depth of approximately 0.45 m in the centre and 0.15 m at the sides. The space between the sleepers is filled with shingle, which does not support the sleepers but provides drainage and a flat surface for evacuation in case of emergencies. The rails are not supported by rail pads and the resilience is mainly provided by the local resilience of the timber sleeper, which has a stiffness of approximately 70 kN/mm.

Rail receptance measurements have been performed in an unloaded track condition by applying lateral and vertical excitations to the rail head at three positions, directly over the sleeper and at mid-span between sleepers. Two instrumented hammers have been used to improve the accuracy of the frequency response and to cover the frequency range up to 5 kHz: a relatively big hammer with an effective mass of 4.218 kg and a soft plastic tip, covering the frequency range up to 1 kHz, and a smaller hammer with an effective mass of 0.646 kg with a harder tip, covering the frequency range up to 5 kHz at lower force levels. Fig. 3 shows the vertical rail receptance measured over the sleeper and at mid-span between sleepers; the latter curve clearly shows a pinned–pinned resonance frequency of 380 Hz [3]. The theoretical pinned–pinned resonance frequency for the London Underground conventional track with Bullhead rail and sleeper spacing of 0.95 m is around 465 Hz.

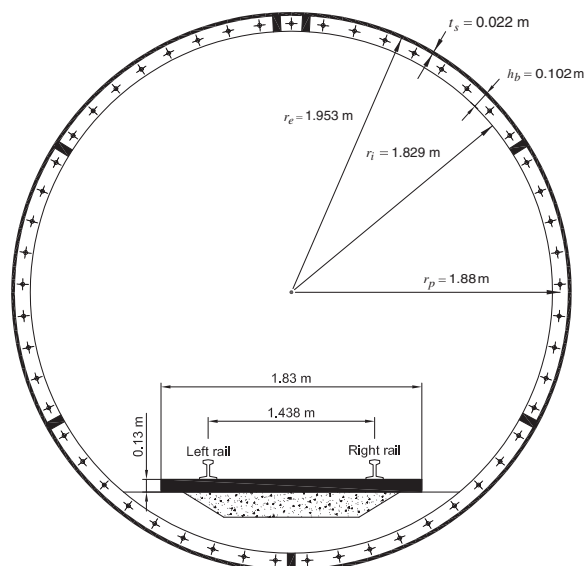


Fig. 2. Cross section of the Bakerloo line tunnel of London Underground at Regent's Park.

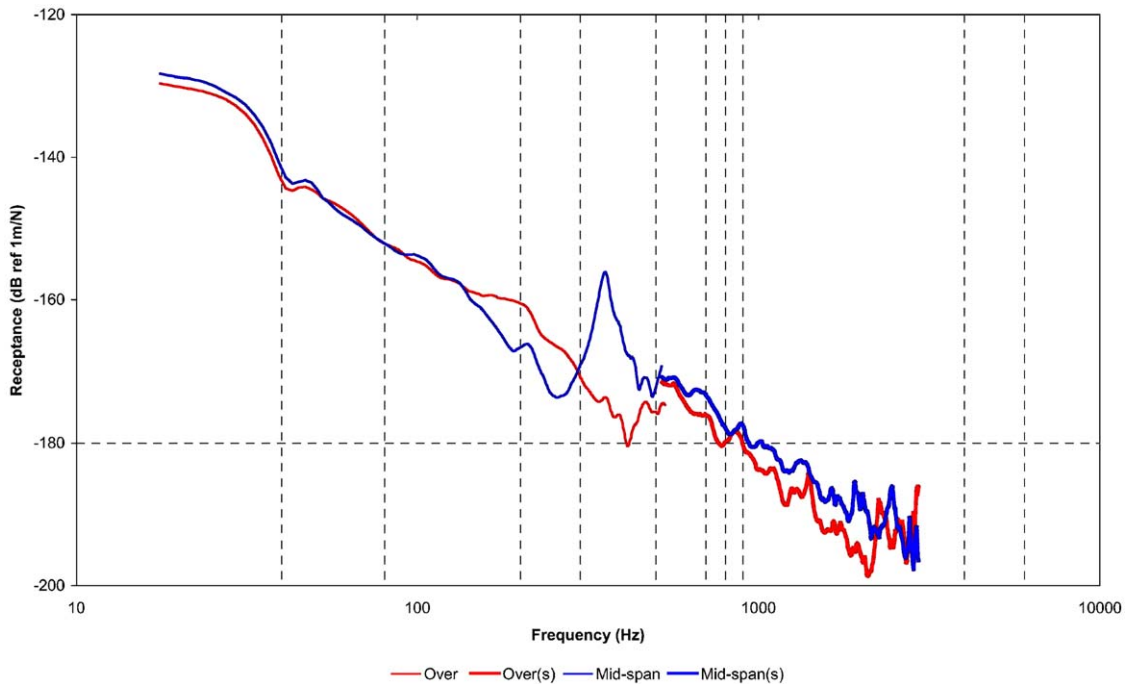


Fig. 3. Vertical rail receptance measured on the right rail.

The same equipment has also been used for wave decay rate measurements. The point of application of the force was moved in steps along the rail away from the fixed position at which the response was measured. A large and a small hammer have been used to obtain a wide and precise frequency response function up to 5 kHz. Two response functions have been measured, one over the sleeper and the other at mid-span, but no significant difference between the two has been observed. The wave decay rate has been determined by considering the one-third octave band spectra of the response functions measured for different distances along the rail.

### 3. Characteristics of the rolling stock

The test train is a normal refurbished 1972 passenger train, consisting of seven cars: a driving motor car (3550), a trailer car (4550), two non-driving motor cars (3450), two trailer cars and a driving motor car (3256). The length of a motor car is 16.09 m, while the length of a trailer car is 15.98 m. The bogie and axle distances on all cars are 10.34 and 1.91 m, respectively. The total length of the test train is 112.29 m, while the distance between the first and the last axle of the train is 108.33 m. The wheels are of the monobloc type and have a diameter of about 0.70 m. The tare mass of a motor car is 15,330 kg, while the bogie mass is 6690 kg and the mass of a wheelset is 1210 kg. The tare mass of a trailer car is 10,600 kg, while the bogie mass is 4170 kg and the mass of a wheelset is 950 kg.

### 4. Rail and wheel roughness

There are a number of rail joints in the vicinity of the reference section, which are classed by London Underground as tight joints and could generate significant impact forces at the wheel/rail interface. Three rail joints are within a distance of 10 m of the reference section of the track (at 581 m from Regent's Park station), but they were all found to be in a good condition.

Rail roughness was measured after completion of the vibration measurements using Müller BBM rail roughness measurement equipment (RM1200E). Measurements were taken on both rails over 50 m of track, at

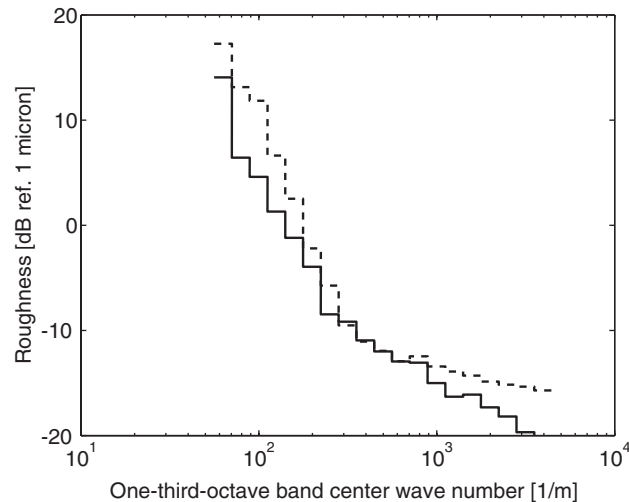


Fig. 4. One-third octave band roughness spectra of the left (solid line) and the right (dashed line) rail, averaged on all positions along the track, as a function of the wavenumber.

seven positions (560, 579, 580, 581, 582, 583, 601 m). At each position, a series of three parallel paths were measured along the centreline of the running band on the rail crown and at  $\pm 10$  mm from this centreline (at position 581 m, two extra parallel paths at  $\pm 5$  mm have also been measured), over a 1-m section centred on the reference position. The data were processed (after removal of spikes and pits) to produce spatial profiles and averaged one-third octave band spectra (based on the 0 and  $\pm 10$  mm positions). Fig. 4 shows the one-third octave band roughness spectra of both rails, averaged over all positions, as a function of the wavenumber  $k_y = 2\pi/\lambda_y$ , with  $\lambda_y$  the corresponding wavelength. The latter varies between values of 0.0016 and 0.10 m, which are relatively short wavelengths that only allow rail roughness-induced vibrations to be assessed above 55 and 138 Hz at train speeds of 20 and 50 km/h, respectively. Unevenness of the rail with a wavelength longer than 0.10 m is undoubtedly present and affects the excitation at lower frequencies, but could not be measured with the available equipment.

Wheel roughness has been measured on both wheels of three wheelsets. For each wheel, measurements were made at the reference position 0 mm (70 mm from the wheel flangeback) and at  $-10$  mm (towards the flange) and  $+10$  mm (towards the field side) from the reference position. The data were processed (after the removal of spikes and pits) to produce one-third octave band spectra per wheel, averaged on the 0 and  $\pm 10$  mm positions. Fig. 5 shows the average one-third octave band roughness spectra on both wheels of wheelset B of the trailer car. Wavelengths obtained vary between 0.0032 and 0.20 m and generate vibrations above 27 and 69 Hz at train speeds of 20 and 50 km/h, respectively. The train was particularly chosen to have good condition wheels. However, wheel 5 on wheelset C was found to have a small flat with a length in the order of 20–30 mm.

Comparing Figs. 4 and 5, the combined roughness of the rails and the wheels is dominated by the rail roughness at low wave numbers, while wheel roughness dominates at the higher wave numbers. The low wave numbers correspond to longer wavelengths and are responsible for excitation in the frequency range of interest for vibrations in buildings (1–80 Hz); higher wave numbers are important for higher frequency excitation that may give rise to re-radiated noise in buildings in the frequency range up to 200–250 Hz. No rail unevenness with a wavelength longer than 0.1 m could be measured with the available equipment, restricting the analysis to frequencies above 55 and 138 Hz for train speeds of 20 and 50 km/h, respectively.

## 5. Dynamic soil characteristics

Historical borings and geological maps of London show that the average thickness of the London clay layer at the site is 40 m.

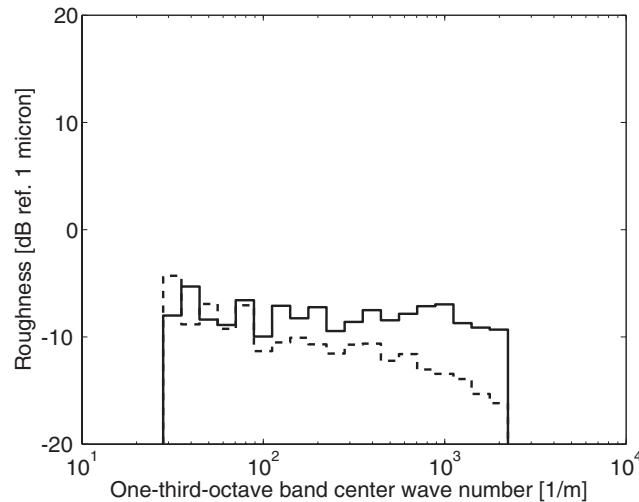


Fig. 5. One-third octave band roughness spectra of the right (solid line) and the left (dashed line) wheel on wheelset B (90815), averaged on three positions (0 and  $\pm 10$  mm) on the wheel.

Cone penetration tests (CPT) were performed at the points FF02, FF04 and FF09 (Fig. 14) up to a depth of 21 m [5]. The soil is clay over the entire depth. A shallow top layer with a thickness of 4–6 m was found to be not very homogeneous with inclusions of sand and gravel and varying cone resistance. The deep layer is very homogeneous, with a cone resistance gradually increasing from 2 MPa at 6 m depth to 3.8 MPa at 21 m depth.

Undisturbed samples have been taken at the points FF02, FF04, FF07 and FF09 at a shallow depth of 4–6 m in the top layer and at depths of 6–7 and 7–7.5 m in the deeper layer. Laboratory tests have been performed to classify the soil and determine the volumetric mass, particle distribution and Atterberg limits [5]. These tests confirm that the soil is saturated clay with inclusions of sand, loam and gravel in the inhomogeneous top layer. The density of the saturated soil is uniform in depth with a mean value of  $1980 \text{ kg/m}^3$ .

Bender element tests have been performed on undisturbed samples (obtained at the same depths as mentioned above), at several confining pressures [5], resulting in an average shear wave velocity of 124 m/s and a longitudinal wave velocity of 1604 m/s, corresponding to a saturated soil with a high Poisson's ratio of 0.497. The material damping ratio is defined as  $\beta = (2Q)^{-1}$ , with  $Q$  the quality factor; values of 0.042 in the top layer and 0.039 in the second layer have been determined by means of free torsion pendulum tests [5].

SCPT at the points FF02, FF04 and FF09 down to a depth of 21 m confirmed the presence of a shallow stiffer layer with a thickness of 4–6 m and a shear wave velocity of 325 m/s on top of a homogeneous halfspace with an average shear wave velocity of 220 m/s [5]. The latter has the same order of magnitude as the value of 251 m/s reported by Bovey [17]. SASW tests in directions parallel and perpendicular to the tunnel confirmed these findings and revealed the presence of a homogeneous clay layer with a shear wave velocity between 200 and 260 m/s [6].

## 6. Axle box response

Axle box vibrations have been measured on six axle boxes during the whole journey of the test train on the inter-station section between Regent's Park and Baker Street stations. Kistler 8702B100 (100 g) accelerometers were mounted on the axle boxes and the vertical acceleration was measured with a sampling frequency  $f_s = 6000.6 \text{ Hz}$ . The measurement period  $T$  depends on the speed of the train.

A fifth-order Butterworth time window is applied between  $0.01T$  and  $0.99T$  in order to smoothen the noise at the beginning and end of the time period  $T$ . This is followed by a third-order Chebyshev band-pass filter with a high-pass frequency  $f_h = 2 \text{ Hz}$ , a low-pass frequency  $f_l = 2999.3 \text{ Hz}$  and a ripple of 0.1 dB in order to remove the DC component and to avoid drifting of the signal.

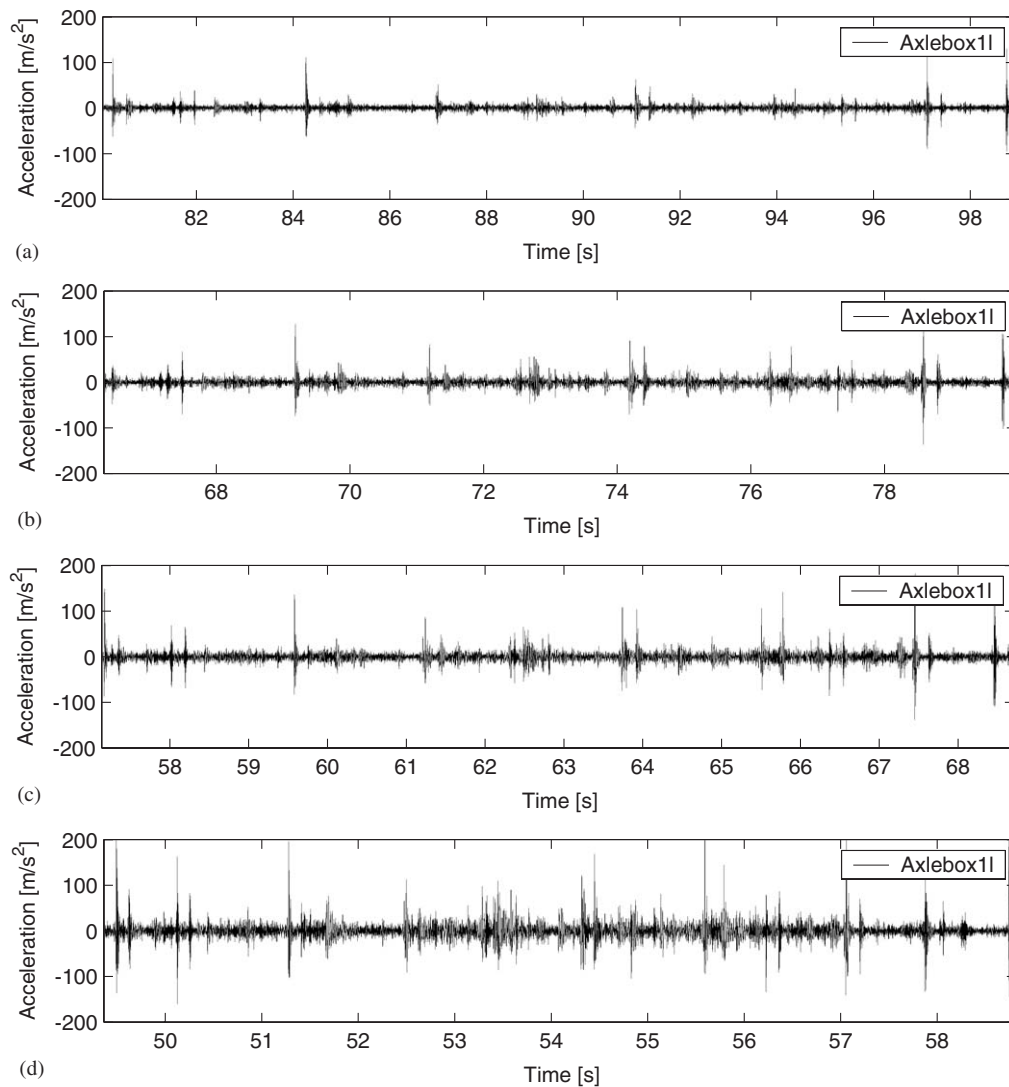


Fig. 6. Time history of the vertical acceleration on axle box 1 for a period of time corresponding to the passage of a train length over the test section at train speeds (a) 23.86 (b) 33.96, (c) 38.88 and (d) 47.60 km/h.

The track form close to Regent's Park station consists of BS 113A flat-bottom rail and is heavily corrugated, producing high levels of axle box acceleration in the first part of the time history [2,18]. An electronic light beam with a response time of 3 ms was positioned above axle box 1, and a reflector was positioned on the tunnel wall at 1 m from the reference section on the track, allowing for synchronisation between the axle box and the track vibration measurements. Fig. 6 shows the time history of the acceleration of axle box 1 for a period of time corresponding to the passage of approximately one train length (rounded to 125 m) over the test section. The average speed of the train was estimated from the track deflection response between the passage of the first and the last axle [18]. The horizontal time axes on Fig. 6 are directly linked to the distance along the track, centred at the reference position. In Fig. 6a, for example, axle 1 passes the reference section at  $t = 89.5$  s. The axle box response is affected by the combined rail and wheel roughness, although the peaks in the response are clearly due to the passage of the axle over the joints in the rail. The passage of axle 1 over the joints of the right rail can be observed (some rail damage was also detected on the right rail in the immediate vicinity of the reference section), as well as the effect of through axle coupling when the same wheelset B is

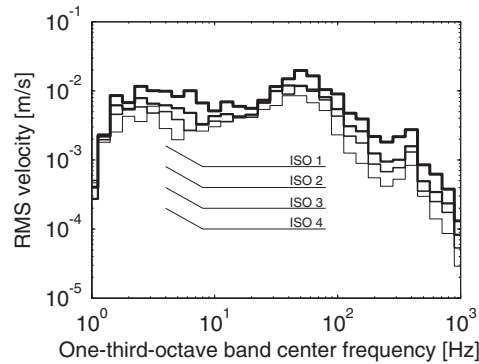


Fig. 7. One-third octave band RMS spectra of the vertical velocity of axle box 1 for a period of time corresponding to the passage of a train length over the test section at train speeds: — 23.86 km/h, — 33.96 km/h, — 38.88 km/h and — 47.60 km/h. Thicker lines are used for increasing train speed.

excited by rail joints on the left rail. There is also a moderate coupling between both axes on a same bogie, a phenomenon which is referred to as leakage: axle 1 is also excited by the passage of axle 2 on the right rail.

The accelerations are integrated to obtain velocity time histories, on which a similar Butterworth time window and Chebyshev filter are applied. Fig. 7 shows the one-third octave band RMS spectra of the vertical velocity of axle box 1 for a period of time corresponding to the passage of a train length over the test section. Independent of the train speed, these spectra reveal maxima in the response around 80 Hz and 380 Hz. The first frequency corresponds to the resonance frequency of the track, which has been measured on the London Underground network with similar track form [2,18]. The second peak around 380 Hz corresponds to the pinned–pinned frequency of the rail between two sleepers, which has also been revealed by the rail receptance measurements (Fig. 3).

The response level increases for increasing train speed. This is explained by the fact that the response at a certain (fixed) frequency  $f = v/\lambda_y$  is caused by longer wavelengths  $\lambda_y$  in the combined rail and wheel roughness spectrum when the train speed  $v$  increases; Fig. 4 clearly shows that the rail roughness spectrum increases for decreasing wavenumber  $k_y$  or increasing wavelength  $\lambda_y$ . Peak accelerations on the axle boxes of the train, determined over a period of time corresponding to the passage of the train over the test section, reveal an almost linear increase with the train speed; an overall increase in peak acceleration of 4–5 dB has been noted for doubling of the train speed [2,18].

## 7. Response of the track and the tunnel

Fig. 8 gives an overview of all accelerometers installed on the track, the tunnel invert and the tunnel wall.

The sampling frequency is equal to  $f_s = 6000.6$  Hz. A signal length  $T = 30.034$  s is sufficiently long to capture each train passage. A fifth-order Butterworth time window is applied between  $0.03T$  and  $0.97T$ , followed by a third-order Chebyshev band-pass filter with a high-pass frequency  $f_h = 4$  Hz, a low-pass frequency  $f_l = 2999.3$  Hz and a ripple of 0.1 dB in order to remove the DC component and to avoid drifting of the signal. Spurious peaks (e.g. due to electrical noise) in the frequency content of the response are removed by subtracting the projection of the acceleration time history on a harmonic function with a frequency  $f_e$  (50 and 100 Hz) within subsequent intervals of  $N_e = 8192$  data samples. The accelerations are integrated to obtain velocity time histories, on which a similar Butterworth time window and Chebyshev filter are applied.

According to the German standard DIN 45672-2 [19], one-third octave band RMS spectra of the response are computed on a reference period  $T_2$ , corresponding to a single train passage, during which the response is considered to be stationary. The running RMS acceleration is calculated with a time window  $T_a = 5$  s. The interval  $T_1$  is subsequently defined as the interval of 4 s centred about the maximum value of the running RMS acceleration. The maximum acceleration  $a_{\max} = \max(a(t))$  is computed in the interval  $T_1$  and the interval  $T_2$  is



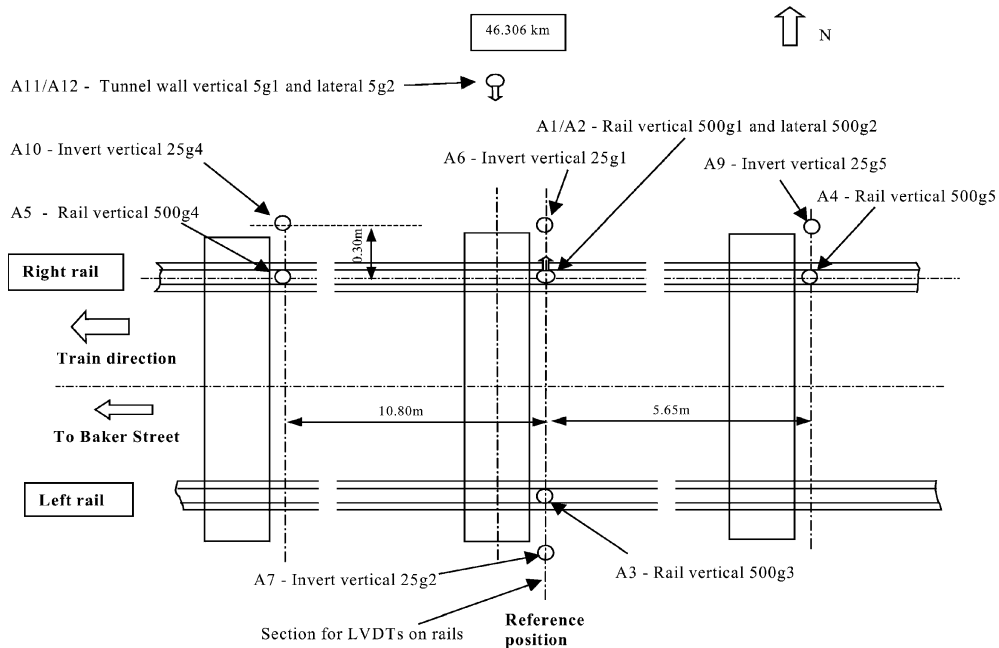


Fig. 8. Measurement setup in the tunnel.

finally determined as the extension of  $T_1$  so that the acceleration does not exceed a value of  $a_{\max}/4$  during a period  $T_b = 2$  s.

Fig. 9 shows the time history of the vertical velocity on the foot of the right rail (A5) during the passage of the test train at four speeds. The response level increases with the train speed. The contribution of each axle can clearly be distinguished, resulting in a quasi-discrete spectrum at low frequencies governed by the bogie and axle distances and the train speed. The increase of the response with the train speed is confirmed in Fig. 10, showing the peak particle velocity in the vertical direction at four points on the rail as a function of the train speed.

Fig. 11a shows the one-third octave band RMS spectra of the vertical velocity at the foot of the rail (A5), and confirms the increasing rail response for increasing train speed. Track resonance around 80 Hz is still observable.

Fig. 12 shows the time history of the vertical velocity on the tunnel invert (A10), for which similar observations can be made. Whereas individual axles can still be differentiated on the tunnel invert, this is no longer the case on the tunnel wall, which is due to the relative attenuation of the higher frequencies in the response for increasing distance to the rails.

One-third octave band RMS spectra of the vertical velocity at the tunnel invert (A10) and the tunnel wall (A11) are shown in Figs. 11b and c for four train speeds. Superimposed on these graphs are limiting curves for work shops, office buildings, residential buildings and operating theatres as specified in the ISO 2631-2 norm for human body exposure to vibrations [20] and the ISO 10137 norm for building vibration with respect to human response [21]. These limiting curves are only shown as a reference order of magnitude that can be helpful to interpret the vibration levels, while it is well understood that the above norms are never used to assess allowable vibration levels in tunnels. Fig. 11b still shows a dependence of the response of the tunnel invert on the train speed; to a lesser extent, this is also the case at the tunnel wall (Fig. 11c). RMS values decrease on the tunnel wall, especially at higher frequencies. Fig. 11d shows the response at the point FF06z at the soil's surface, 28 m above the tunnel; it must be noted that the latter data are affected by a low-pass anti-aliasing filter at 125 Hz. Fig. 13 confirms that, unlike the response on the tunnel wall (A11), the free field response above the tunnel (FF06) only weakly depends on the train speed. The results in Fig. 11 demonstrate

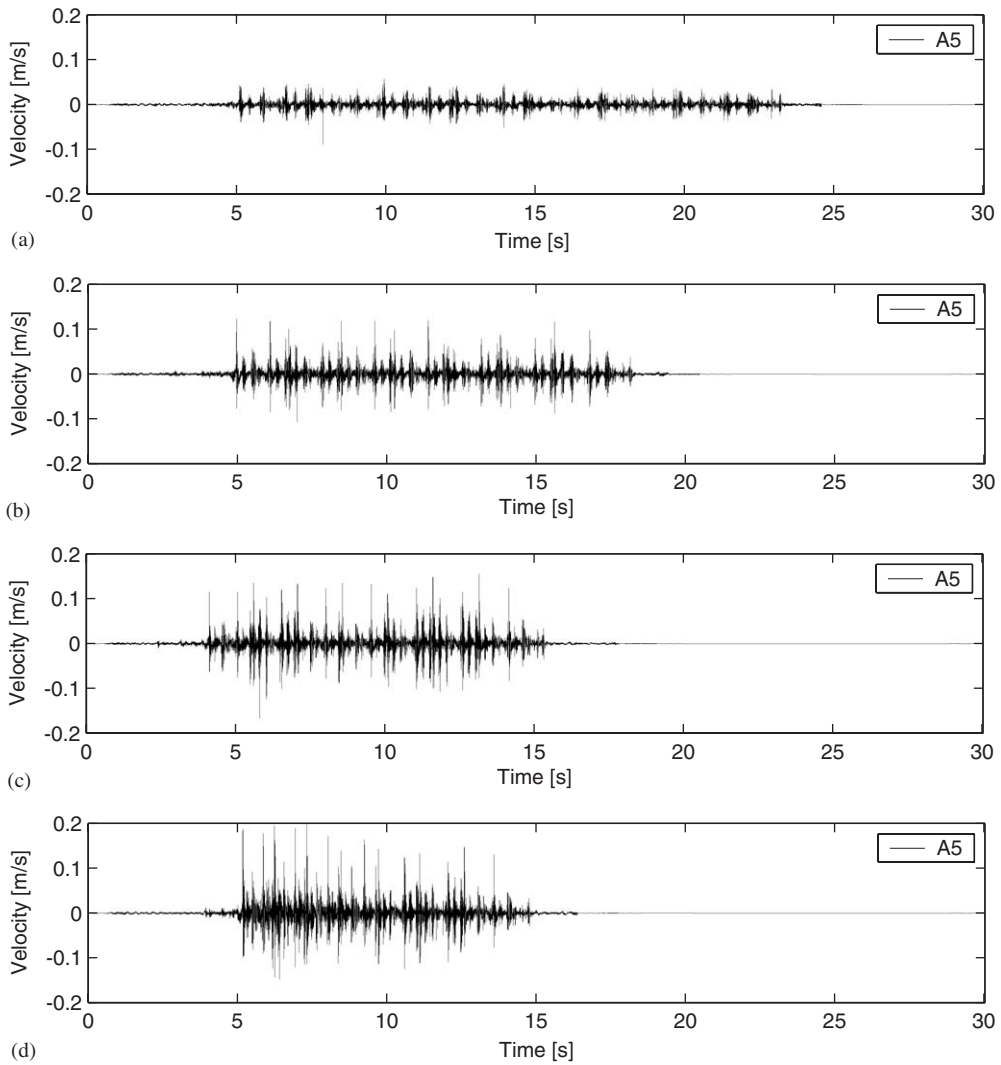


Fig. 9. Time history of the vertical velocity on the rail (A5) for the passage of the test train at speeds (a) 23.86, (b) 33.96, (c) 38.88 and (d) 47.60 km/h.

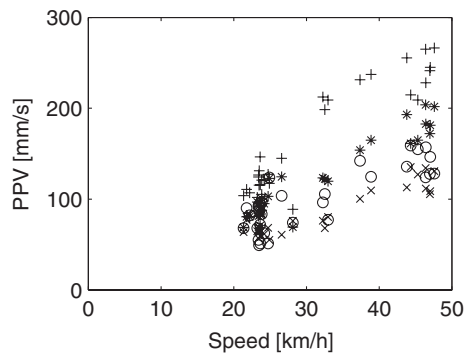


Fig. 10. Vertical (○A1; ×A3; +A4; \*A5) PPV on the rail as a function of the train speed.

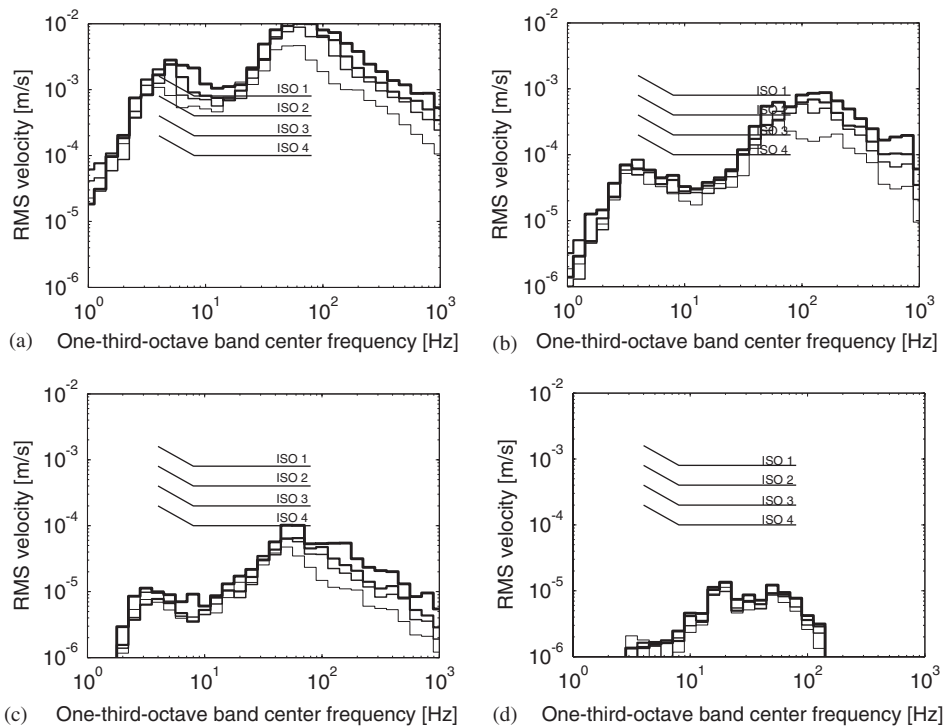


Fig. 11. One-third octave band RMS spectra of the vertical velocity on (a) the rail (A5), (b) the tunnel invert (A10), (c) the tunnel wall (A11), and (d) the free field (FF06z) at train speeds: — 23.86 km/h, — 33.96 km/h, — 38.88 km/h and — 47.60 km/h. Thicker lines are used for increasing train speed.

that the vibration amplitudes decrease and the frequency content shifts towards lower frequencies for increasing distance from the track.

## 8. Response in the free field

In the free field, vibrations have been measured on two measurement lines in Regent's Park, perpendicular to the Bakerloo line tunnel. Fig. 14 shows the location of the tunnel, the measurement lines 1 and 2 in the free field and the buildings at 17 and 25 York Terrace West. A right-handed Cartesian frame of reference is defined with the origin at the free surface above kilometre post 46.306 of the north-bound Bakerloo line, the  $x$ -axis perpendicular to the tunnel axis, the longitudinal  $y$ -axis in the direction of the tunnel and the  $z$ -axis pointing upwards. Reference line 1 corresponds to the  $x$ -axis ( $y = 0$ ) and is situated opposite the building at 17 York Terrace West, while line 2 is parallel to line 1 and located at  $y = -32.5$  m, opposite the building at 25 York Terrace West.

Simultaneous vibration measurements have been performed in the free field and in both buildings using three data acquisition (DAQ) systems.

- (1) Measurements in the free field have been performed with a first DAQ system with 20 channels. Five points are located at the surface: three along line 1 (FF01, FF02, FF04) and two along line 2 (FF07 and FF09), where vertical and horizontal (in the  $x$ -direction) accelerations have been measured, except at the points FF01 and FF09, where only vertical accelerations are measured. High-sensitivity Sundstrand 700 linear servo accelerometers are mounted on an aluminium block with a long peg that is driven into the ground. Furthermore, tri-axial measurements have been performed at a depth of 15 m below the surface at two locations along line 1 (FF03 and FF05) and line 2 (FF08 and FF10), using tri-axial Sundstrand 800 accelerometers installed in a seismic cone that is pushed into the ground.

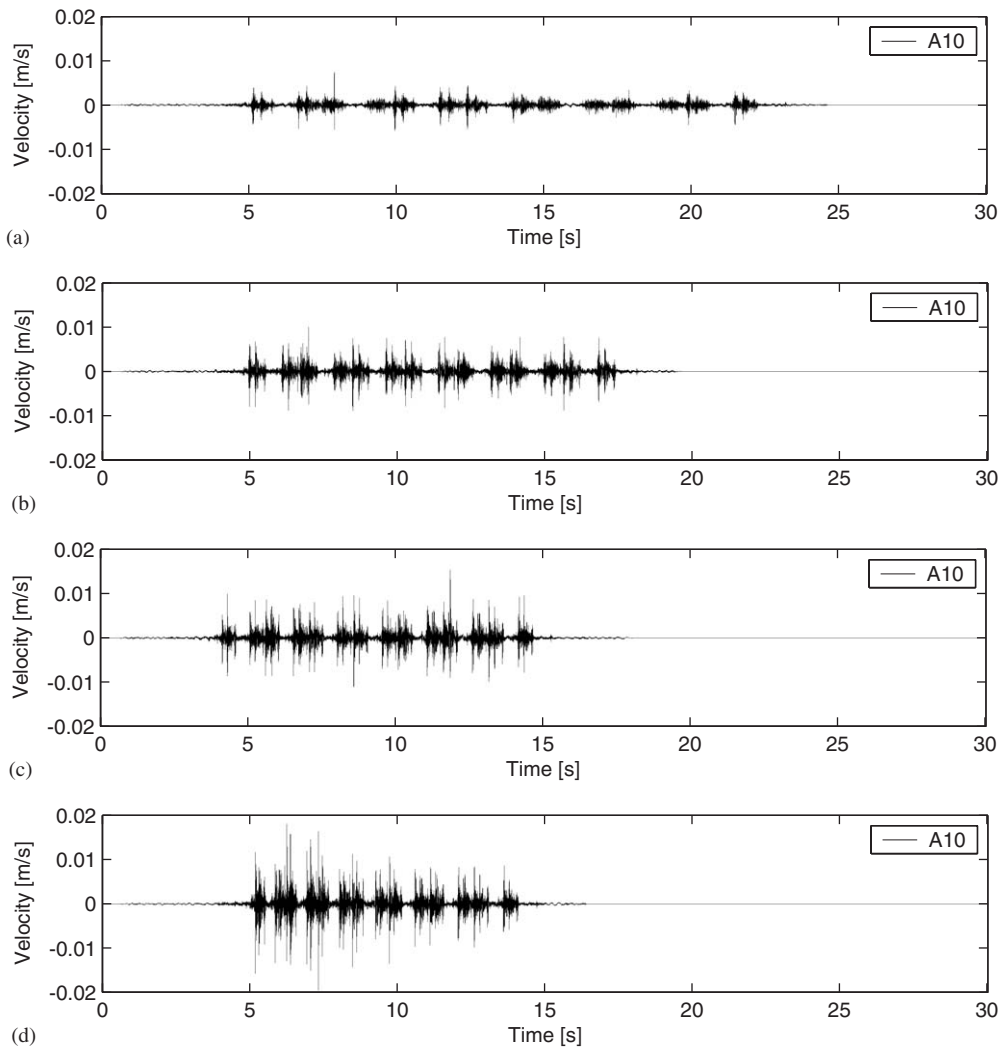


Fig. 12. Time history of the vertical velocity on the tunnel invert (A10) for the passage of the test train at speeds (a) 23.86, (b) 33.96, (c) 38.88 and (d) 47.60 km/h.

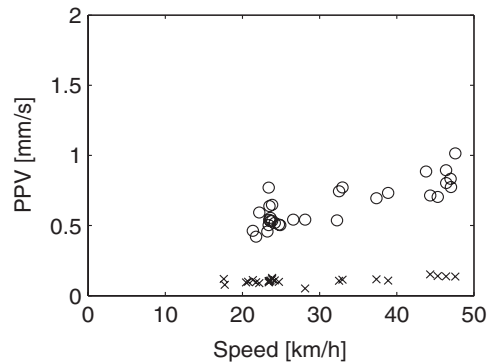


Fig. 13. PPV on the tunnel wall (○A11) and in the free field (× FF06z) as a function of the train speed.

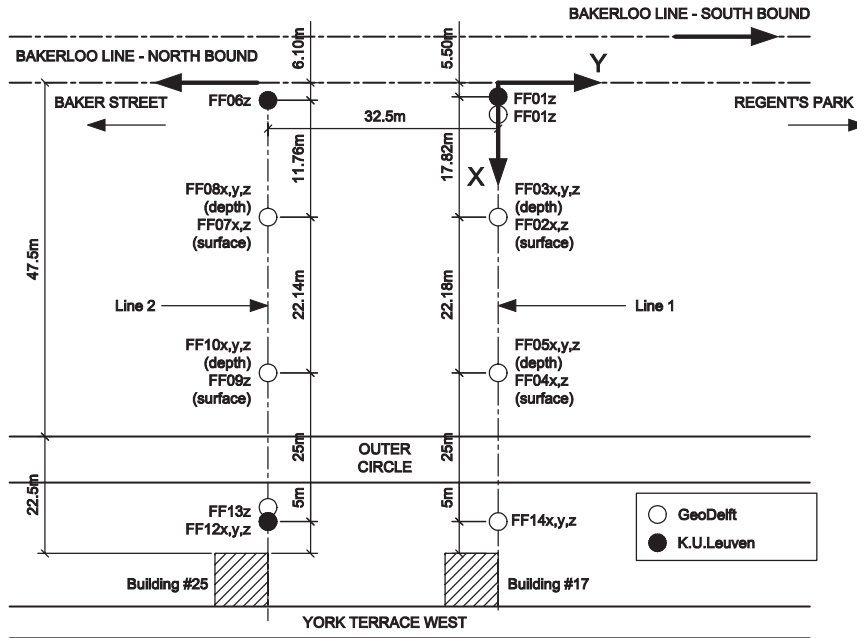


Fig. 14. Measurement setup in the free field.

- (2) A 16-channel DAQ system has been used for vibration measurements in the building at 25 York Terrace West, using 1 and 10 V/g high-sensitivity seismic PCB accelerometers and a low-pass anti-aliasing filter with a cut-off frequency of 125 Hz. The vertical acceleration was also measured at the point FF01 in the reference section above the tunnel, for synchronization with the free-field measurements, as well as in three directions at the point FF12 in front of the building. The results of the vibration measurements in this building will be discussed in the following section.
- (3) Measurements in the building at 17 York Terrace West have been performed using a 10-channel DAQ system using 1 V/g accelerometers, including a tri-axial measurement at the point FF14 in front of the building, as well as the measurement of the vertical acceleration at the point FF13, next to the point FF12 in front of the building at 25 York Terrace West, in order to synchronize the measurements in both buildings.

The present paper focusses on results measured in the free field along line 2 and in the building at 25 York Terrace West. The sampling frequency is  $f_s = 500$  Hz and the signal length is  $T = 65.536$  s. A fifth-order Butterworth time window is applied between  $0.01T$  and  $0.99T$ , followed by a third-order Chebyshev band-pass filter with a high-pass frequency  $f_h = 2$  Hz (free-field data) or  $f_h = 4$  Hz (building data), a low-pass frequency  $f_l = 249$  Hz and a ripple of 0.1 dB. Spurious peaks at 50 and 100 Hz are removed using a similar procedure as for the track and tunnel vibration data. The accelerations are integrated to obtain velocity time histories, on which a similar Butterworth time window and Chebyshev filter are applied. One-third octave band RMS velocity spectra are computed according to the German standard DIN 45672-2 [19].

Fig. 15 illustrates that the dependence of the horizontal and vertical PPV on the train speed is moderate to low. The vertical PPV on the free surface above the tunnel (FF06z) is lower than at a depth of 15 m, at a lateral distance of approximately 18 m from the tunnel (FF08z), as the latter point is closer to the tunnel. The passage of individual axles and bogies can no longer be identified in the time history of the response, as was also the case on the tunnel wall, and is not presented here. At depth, the horizontal PPV is generally lower than the vertical PPV (FF08 and FF10), while both components have the same order of magnitude at the surface (FF07 and FF12), which is probably due to amplification of vertically propagating waves through the layered soil. At

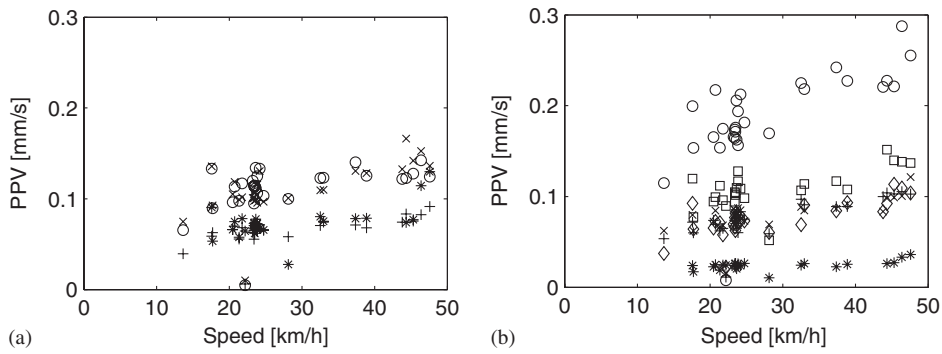


Fig. 15. (a) Horizontal ( $\circ$ FF08x;  $\times$ FF07x;  $+$ FF10x;  $*$ FF12x) and (b) vertical ( $\square$ FF06z;  $\circ$ FF08z;  $\times$ FF07z;  $+$ FF10z;  $\diamond$ FF09z;  $*$ FF12z) PPV in the free field as a function of the train speed.

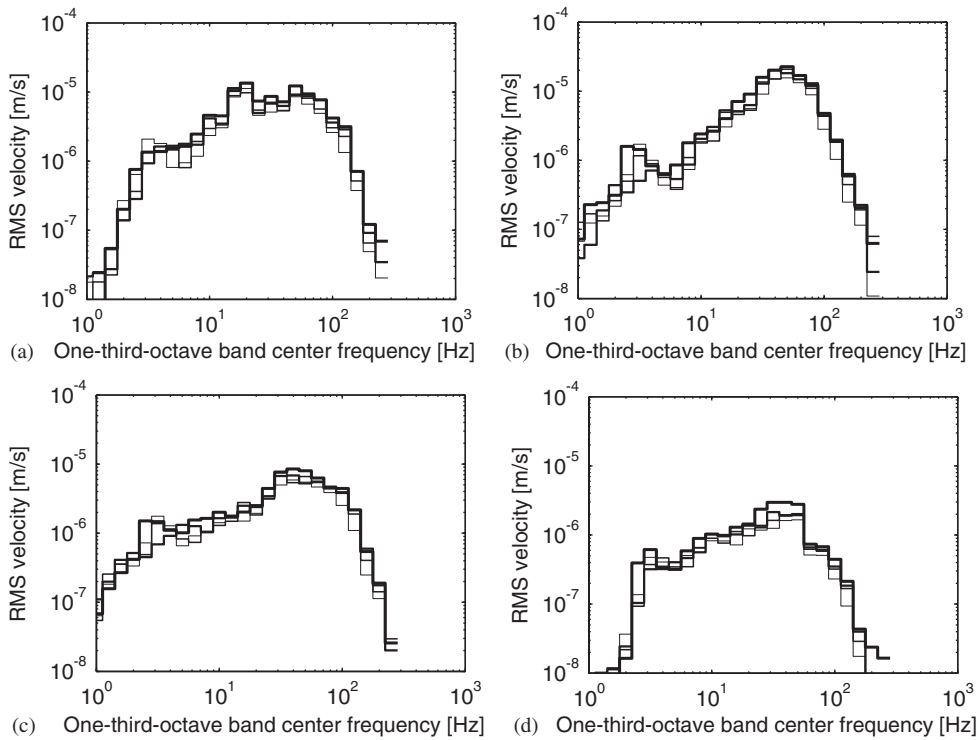


Fig. 16. One-third octave band RMS spectra of the vertical velocity in the free field at (a) FF06z, (b) FF08z, (c) FF07z, and (d) FF12z at train speeds — 23.86 km/h, — 33.96 km/h, — 38.88 km/h and — 47.60 km/h. Thicker lines are used for increasing train speed.

all measurement points at the surface, the PPV is below the threshold for human perception, which is commonly defined as 0.3 mm/s [22].

The moderate to low dependence of the vibration on the train speed is confirmed in Fig. 16, showing the one-third octave band RMS spectra of the vertical velocity at four points in the free field for four different train speeds. The frequency content is mainly governed by wheel and rail unevenness and the maximum level is situated between 15 and 60 Hz for the lower train speeds and shifts up to 80 Hz at higher train speeds. Low-frequency components associated with the passage of the individual axles can no longer be distinguished. Amplitudes decrease for increasing distance from the tunnel due to geometric damping, while higher frequency components at increasing distance are significantly attenuated by material damping in the soil.

9. Response in the building

Fig. 17 shows the location of accelerometers in the building at 25 York Terrace West. Tri-axial measurements have been performed in the garden in front of the building (FF12) and in the basement (BA01). Furthermore, vertical accelerations were measured at mid span on the slab of the first floor (F002z) and at mid span on a stiffening beam under the slab (F003z). Horizontal accelerations have also been measured in the *x*- and *y*-direction at the base of a concrete column on the three floors of the building. Complementary measurement points were installed in the free field on top of the tunnel (FF01z, FF06z) for synchronization, triggering and identification of trains on the north-bound Bakerloo line. The same data analysis procedure has been used as for the free-field data.

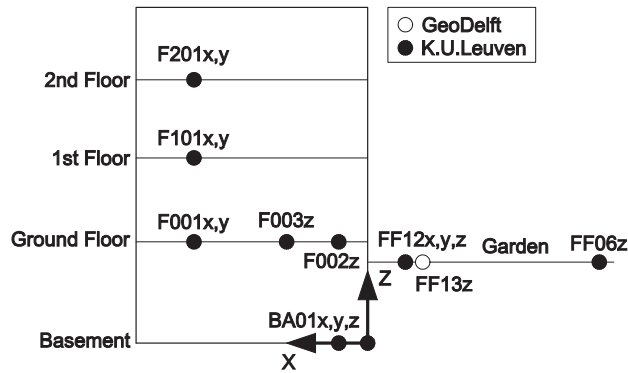


Fig. 17. Position of the accelerometers in the building at 25 York Terrace West.

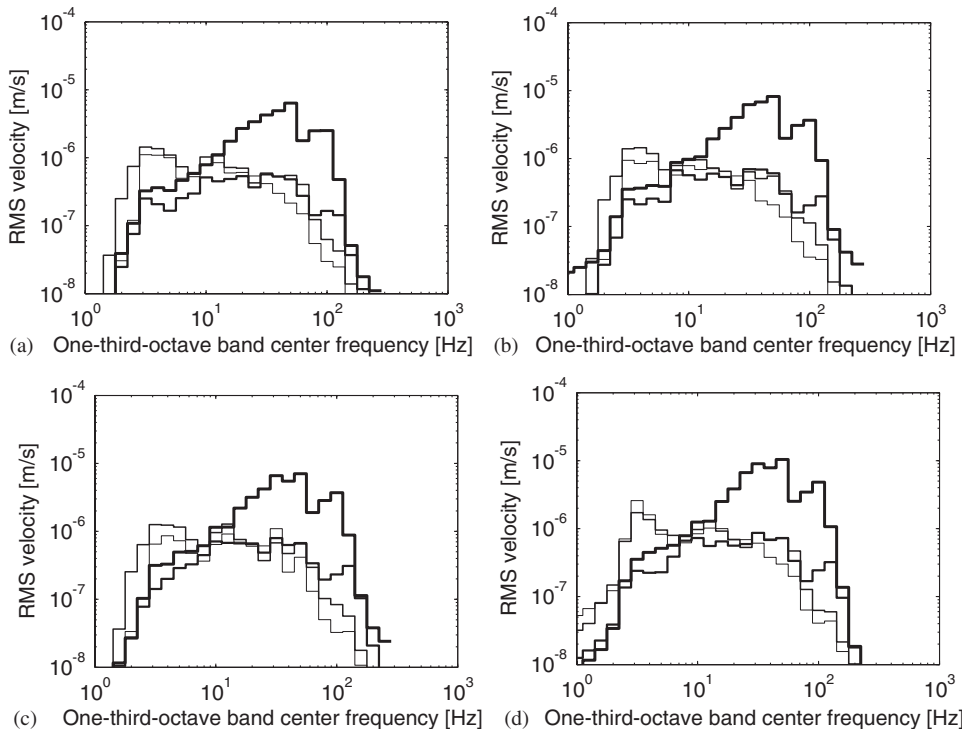


Fig. 18. One-third octave band RMS spectra of the horizontal velocity in the building (— FF12x, — BA01x, — F101x, — F201x; decreasing line thickness) at train speeds (a) 23.86, (b) 33.96, (c) 38.88 and (d) 47.60 km/h.

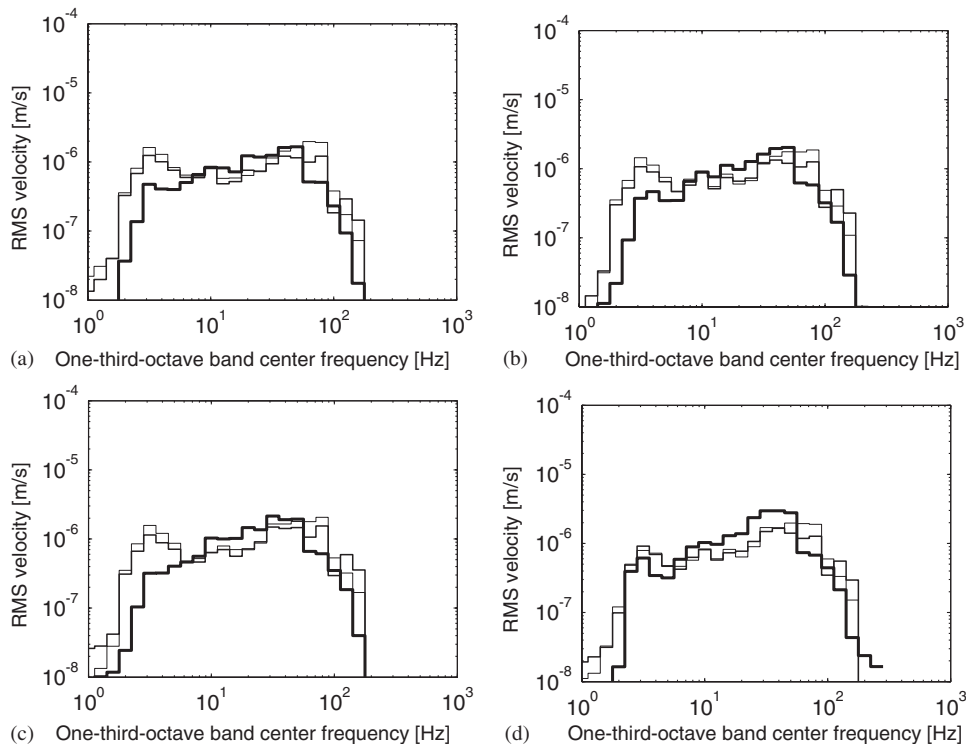


Fig. 19. One-third octave band RMS spectra of the vertical velocity in the building (— FF12z, — BA01z, — F002z, — F003z; decreasing line thickness) at train speeds (a) 23.86, (b) 33.96, (c) 38.88 and (d) 47.60 km/h.

Analysis of the time history of the horizontal and vertical response in the building revealed that the peak response in the horizontal  $x$ -direction and the vertical  $z$ -direction at several points in the building only very moderately increases with the train speed. Vibration levels in the building are very low and well below 0.1 mm/s.

Figs. 18 and 19 show the one-third octave band RMS spectra of the horizontal and vertical velocities, respectively, at different points in the building for four different speeds of the train. These figures confirm a very moderate dependence of the response on the train speed.

The horizontal component is considerably reduced between the free field and the basement, especially between 10 and 100 Hz, as confirmed by Fig. 20a, where the transfer function, defined as the difference between the one-third octave band spectra (averaged over four train passages), is shown. Moderate amplification on the second storey is found in the low-frequency range around 2 Hz (Fig. 20b), which is probably related to the overall lateral bending modes of the building, while moderate amplification is still found below 30 Hz. The vibrations are reduced at higher frequencies.

The analysis of vertical components is limited to the free field (FF12z) and two points on the slab on the ground floor, where F002z is located at mid span on a flexible slab and F003z is at mid span above a stiffening beam under the slab. Due to malfunctioning of an accelerometer, however, no vertical vibration transfer between the free field and the basement nor between the basement and the slab can be assessed. Fig. 20c shows the averaged transfer function between the slab on the ground floor and the free field. No amplification is found in the frequency range between 20 and 40 Hz where slab resonance is usually expected. The slab vibrations are generally lower than in the free field, which is due to significant prior reduction at basement level. Amplification in the frequency range between 60 and 90 Hz can be related to floor resonance at higher bending modes. Amplification in the higher frequency range above 100 Hz is probably spurious and due to the mounting of the accelerometers on a stiff steel plate with three adjustable screws, rather than to structural resonance.



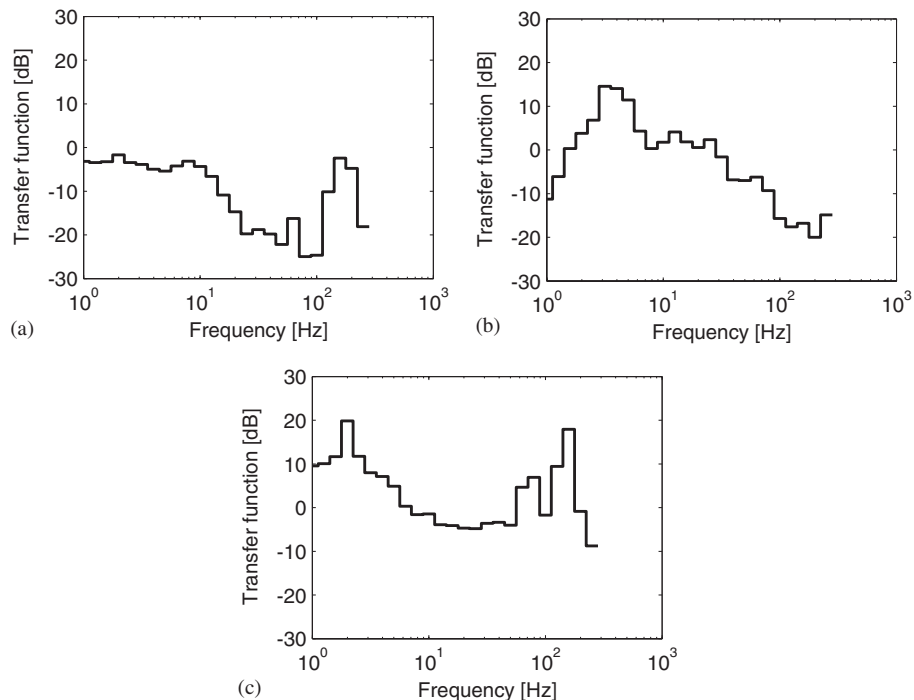


Fig. 20. One-third octave band spectra of (a) the horizontal transfer functions between the basement (BA01x) and the free field (FF12x) and (b) the second storey (F201x) and the basement (BA01x), and (c) the vertical transfer function between the slab on the ground (F002z) and the free field (FF12z), averaged for four train speeds.

## 10. Conclusion

Elaborate vibration measurements have been made during 35 passages of a test train at speeds varying between 20 and 50 km/h in the north-bound Bakerloo line tunnel in Regent's Park, London. Vibration measurements have been performed on the axle boxes of a trailer car of the test train, on the rails, on the tunnel invert and tunnel wall, in the free field (both at the surface and at depth) and in two buildings at 70 m from the tunnel. Wheel and rail roughness have been measured and the dynamic characteristics of the track and the soil have been determined by independent dynamic tests prior to the vibration measurements.

Vibrations have been analysed in terms of acceleration or velocity time histories, peak acceleration and velocity, as well as one-third octave band rms velocity spectra and transfer functions in the building. The following conclusions can be drawn from the present analysis:

- (1) The combined roughness of the rails and the wheels is dominated by the rail roughness at low wavenumbers, corresponding to longer wavelengths, while wheel roughness dominates the combined roughness at the higher wavenumbers. No wavelengths of the rail unevenness longer than 0.1 m could be measured with the available equipment, restricting the analysis to frequencies above 55 and 138 Hz for train speeds of 20 and 50 km/h, respectively. Accounting only for the effect of rail roughness, increasing the train speed at a particular frequency results in a higher excitation originating from a larger unevenness at a lower wavenumber or longer wavelength.
- (2) The axle box response is also considerably dominated by transient excitation at rail joints, which increases almost linearly with train speed. An increase of about 4–5 dB was observed for doubling of the train speed. The resonance frequency of the track around 80 Hz and the pinned–pinned frequency of the rail at 380 Hz could clearly be identified from the one-third octave band RMS spectra of the axle box velocity.
- (3) The response of the rails, the tunnel invert and the tunnel wall also increase for increasing train speed, since they are caused by dynamic wheel/rail contact forces, which can be related to the axle box

accelerations. This conclusion follows from the analysis of peak particle velocities and one-third octave band rms velocity spectra as a function of the train speed. Whereas the passage of individual axles could clearly be identified on the rail and the tunnel invert, this is no longer the case on the tunnel wall, which is due to a significant attenuation of the high-frequency components.

- (4) Analysis of PPV and one-third octave band rms spectra of the velocity in the free field shows a moderate to low dependence on the train speed. Geometric and material damping in the soil affect the amplitude and frequency content of the response. At a depth of 15 m, horizontal components are generally lower than the vertical components, whereas they have the same order of magnitude at the surface, which may be due to local site amplification. Vibration levels at the surface are lower than the threshold for human perception.
- (5) Building vibrations were quite low, with a low signal-to-noise ratio even when high-sensitivity seismic accelerometers were used. Horizontal building vibrations are significantly attenuated at basement level in the frequency range between 10 and 100 Hz. Some amplification has been observed on the second storey, which can probably be attributed to lateral bending of the building. Vertical vibrations on a flexible slab on the ground floor do not show amplification with respect to the free-field vibrations in the garden in the frequency range where this would normally be expected.

The experimental data presented here will subsequently be used for the validation of numerical prediction models under development. Model development, calibration and validation will benefit from the available dataset. It is equally true, however, that further interpretation of the vibration data presented here will benefit from the availability of numerical prediction models.

### Acknowledgements

The results presented in this paper have been obtained within the frame of the EC-Growth project G3RD-CT-2000-00381 CONVURT (“The control of vibration from underground railway traffic”). The financial support of the European Community is kindly acknowledged.

### References

- [1] <http://www.convurt.com>, 2003.
- [2] N. Dadkah, Axle box acceleration measurements in London, Regent’s Park—Baker Street, Report R1064, MRCL, July 2003 (CONVURT EC-Growth Project G3RD-CT-2000-00381).
- [3] A. Wang, Track measurements on London Underground Bakerloo Line, Report 16487-2, Pandrol, May 2003 (CONVURT EC-Growth Project G3RD-CT-2000-00381).
- [4] P. Chatterjee, G. Degrande, S. Jacobs, Free field and building vibrations due to the passage of test trains at the site of Regent’s Park in London, Report BWM-2003-20, Department of Civil Engineering, K.U. Leuven, December 2003 (CONVURT EC-Growth Project G3RD-CT-2000-00381).
- [5] P. Hölscher, V. Hopman, Test site Regent’s Park London, Soil description, Report 381540-104, Version 2, GeoDelft, December 2003 (CONVURT EC-Growth Project G3RD-CT-2000-00381).
- [6] L. Pyl, G. Degrande, Determination of the dynamic soil characteristics with the SASW method at Regent’s Park in London, Report BWM-2003-17, Department of Civil Engineering, K.U. Leuven, December 2003 (CONVURT EC-Growth Project G3RD-CT-2000-00381).
- [7] P. Chatterjee, G. Degrande, Free field vibration measurements due to a test train at the site of Cité Universitaire in Paris, Report BWM-2002-09, Department of Civil Engineering, K.U. Leuven, November 2002 (CONVURT EC-Growth Project G3RD-CT-2000-00381).
- [8] S. Jacobs, P. Chatterjee, G. Degrande, Vibrations due to service trains in the ‘Maison du Mexique’ on the RER B line at Cité Universitaire in Paris, Report BWM-2003-02, Department of Civil Engineering, K.U. Leuven, February 2003 (CONVURT EC-Growth Project G3RD-CT-2000-00381).
- [9] P. Chatterjee, G. Degrande, S. Jacobs, J. Charlier, P. Bouvet, D. Brassensx, Experimental results of free field and structural vibrations due to underground railway traffic, in: *10th International Congress on Sound and Vibration*, Stockholm, Sweden, July 2003 (CD-ROM).
- [10] G. Degrande, P. Chatterjee, S. Jacobs, J. Charlier, P. Bouvet, D. Brassensx, CONVURT project—Experimental results of free field and structural vibrations due to underground railway traffic, in: *World Congress on Railway Research*, Edinburgh, UK, September 2003.
- [11] D. Clouteau, M. Arnst, T.M. Al-Hussaini, G. Degrande, Free field vibrations due to dynamic loading on a tunnel embedded in a stratified medium, *Journal of Sound and Vibration* 283 (1–2) (2005) 173–199.

- [12] G. Degrande, D. Clouteau, R. Othman, M. Arnst, H. Chebli, R. Klein, P. Chatterjee, B. Janssens, A numerical model for ground-borne vibrations from underground railway traffic based on a periodic finite element—boundary element formulation. *Journal of Sound and Vibration* (2006), this issue, doi:10.1016/j.jsv.2005.12.023.
- [13] H.E.M. Hunt, M.F.M. Hussein, J.P. Talbot, Insertion loss models for evaluating the performance of vibration countermeasures for underground railways, in: *10th International Congress on Sound and Vibration*, Stockholm, Sweden, July 2003 (CD-ROM).
- [14] M.F.M. Hussein, H.E.M. Hunt, An insertion loss model for evaluating the performance of floating-slab track for underground railway tunnels, in: *10th International Congress on Sound and Vibration*, Stockholm, Sweden, July 2003 (CD-ROM).
- [15] M.F.M. Hussein, H.E.M. Hunt, A power flow method for evaluating vibration from underground railways, *Journal of Sound and Vibration* (2006), this issue, doi:10.1016/j.jsv.2005.12.012.
- [16] M.F.M. Hussein, *Vibration from Underground Railways*, Ph.D. Thesis, Department of Engineering, University of Cambridge, 2005.
- [17] E.C. Bovey, Investigation into vibration transmission from railways at Regent's Park using impact excitation, Report, London Underground, London Transport International Services Limited, December 1981.
- [18] N. Dadkash, A. Wang, Relationship between axle box and trackside vibration at higher frequencies at various speeds in a deep bored tunnel, in: *11th International Congress on Sound and Vibration*, St Petersburg, Russia, 2004, pp. 3063–3070 (CD-ROM).
- [19] Deutsches Institut für Normung. *DIN 45672 Teil 2: Schwingungsmessungen in der Umgebung von Schienenverkehrswegen: Auswerteverfahren*, 1995.
- [20] International Organization for Standardization. *ISO 2631-2:1999: Mechanical vibration and shock—evaluation of human exposure to whole-body vibration—part 2: vibration in buildings (1 to 80 Hz)*, 1999.
- [21] International Organization for Standardization. *ISO 10137:1992: Base for design of structures—serviceability of buildings against vibration*, 1992.
- [22] J.F. Wiss, Construction vibrations: state-of-the-art, *Journal of the Geotechnical Engineering Division, ASCE* 107 (GT2) (1981) 167–181.